

Elsevier Editorial System(tm) for Electrochimica Acta
Manuscript Draft

Manuscript Number:

Title: Formation of graphene oxide nano-disks by electrochemical oxidation of HOPG

Article Type: Research Paper

Keywords: HOPG; electrochemical oxidation of graphite; graphite oxide; STM; intercalation

Corresponding Author: Prof. Koichi Jeremiah Aoki, Ph.D.

Corresponding Author's Institution: University of Fukui

First Author: Koichi Jeremiah Aoki, Ph.D.

Order of Authors: Koichi Jeremiah Aoki, Ph.D.; Hongxin Wang; Jingyuan Chen, PhD; Toyohiko Nishiumi, PhD

Abstract: When HOPG (highly oriented pyrolytic graphite) was electrochemically oxidized in alkali solution, STM observation showed that graphite oxide with homo-sized disks 15 nm in diameter and 0.5 nm in thickness was formed dispersively on the HOPG surface. With an increase in the anodic charge, the number of the disks enhanced, and covered finally the HOPG surface without overlap at the maximum coverage, 70%. The projected area of the disks was proportional to the anodic charge when the charge was small. The disks were hydrophilic. The double layer capacitance of the oxidized HOPG increased slightly with the anodic charge, implying that the disks should be an electrical insulator. The fully disk-coated HOPG did not block the diffusion-controlled current of the redox species. The layer of the disks must be porous for ions or solutions. The formation of the uniform size may be ascribed to the difference between the density of graphite oxide and that of the basal plane of graphite. The formation of nano-disks and their properties are inconsistent with such an image of intercalation that ions are inserted into layers of graphenes of HOPG.

Dear an editor of Electrochimica Acta:

I would like to submit the attached files to Electrochimica Acta as a full paper.

This work has been stimulated by a question about a relationship between the anodic intercalation into HOPG and microscopic surface morphology. A new insight is that the oxidized surface is different from the conventional image of the intercalation.

All the coworkers have agreed with the publication.

Possible reviewers are

1. Dr. C.T.J. Low

Electrochemical Engineering Laboratory,
Energy Technology Research Group,
Faculty of Engineering and the Environment,
University of Southampton,
Highfield, Southampton SO17 1BJ, United Kingdom
E-mail addresses: C.T.J.Low@soton.ac.uk

2. Dr. Horacio J. Salavagione

Instituto de Ciencia y Tecnología de Polímeros (ICTP-CSIC),
C/Juan de la Cierva 3, 28006 Madrid, Spain
fax: +34 915644853
horacio@ictp.csic.es

3. Professor Murat Alanyalioglu

Instituto de Ciencia de Materiales de Barcelona, CSIC,
Campus de la Universidad Autónoma de Barcelona,
E-08193 Barcelona, Spain
Fax: +90 442 2360948.
E-mail address: malanya@atauni.edu.tr

4. Professor Richard L. McCreery

National Institute for Nanotechnology,
Department of Chemistry, University of Alberta, Edmonton,
Alberta T6G 2M9, Canada
e-mail address: mcreery@ualberta.ca

5. Professor Royce W. Murray

Kenan Laboratories of Chemistry,
University of North Carolina, Chapel Hill,
North Carolina
e-mail address: rwm@email.unc.edu

1
2
3
4
5
6
7
8
9
10
11
12
13
14
15
16
17
18
19
20
21
22
23
24
25
26
27
28
29
30
31
32
33
34
35
36
37
38
39
40
41
42
43
44
45
46
47
48
49
50
51
52
53
54
55
56
57
58
59
60
61
62
63
64
65

Formation of graphene oxide nano-disks by electrochemical oxidation of HOPG

Koichi Jeremiah Aoki*, Hongxin Wang, Jingyuan Chen, Toyohiko Nishiumi
Department of Applied Physics, University of Fukui, 3-9-1 Bunkyo, Fukui, 910-0017 Japan

Abstract

When HOPG (highly oriented pyrolytic graphite) was electrochemically oxidized in alkali solution, STM observation showed that graphite oxide with homo-sized disks 15 nm in diameter and 0.5 nm in thickness was formed dispersively on the HOPG surface. With an increase in the anodic charge, the number of the disks enhanced, and covered finally the HOPG surface without overlap at the maximum coverage,70%. The projected area of the disks was proportional to the anodic charge when the charge was small. The disks were hydrophilic. The double layer capacitance of the oxidized HOPG increased slightly with the anodic charge, implying that the disks should be an electrical insulator. The fully disk-coated HOPG did not block the diffusion-controlled current of the redox species. The layer of the disks must be porous for ions or solutions. The formation of the uniform size may be ascribed to the difference between the density of graphite oxide and that of the basal plane of graphite. The formation of nano-disks and their properties are inconsistent with such an image of intercalation that ions are inserted into layers of graphenes of HOPG.

key words: HOPG; electrochemical oxidation of graphite; graphite oxide; STM; intercalation

* corresponding author, e-mail kaoki@u-fukui.ac.jp, phone +81 90 8095 1906, fax +81 776 27 8750

Introduction

Considerable amounts of graphene sheets have been produced through reduction of graphite oxide [1-6], which takes a form of dispersing sheets or flakes in suspensions [6]. Graphite oxide has been generated by chemical oxidation of graphite by oxidants including concentrated sulfuric acid, nitric acid and potassium permanganate based on the Hummers method [7]. It is generally difficult to control a degree or intensity of chemical oxidation. In contrast, an electrochemical technique can control well oxidation by time-variations of voltage or current, and is a promising method of producing graphene oxide with quality control. Electrochemical production of graphene has been developed in the light of scaling-up the process since 2011. The state-of-the-art methods for electrochemical synthesis of graphene have been reviewed, including the properties as well as analytical methods [8].

Electrochemical reactions at graphite electrodes have been directed intensely to intercalation of lithium ion at secondary batteries early in 1980s [9-13]. The electrochemical intercalation has often brought about exfoliation from graphite [14,15]. Graphene is thought to be formed electrochemically in two steps: intercalated ions expand inter-distances among graphene layers into which solvent is penetrated; the penetrated solvent generates electrochemically gasses, which exfoliate graphene layers [8,16]. Although this mechanism is intuitively reasonable enough for explaining the electrochemical exfoliation, voltages and current densities for the interaction and gas evolution have not been quantitatively discussed yet. The quantitative discussion is not easy because there is difficulty in controlling voltages for such high current density that graphene flakes are dispersed in suspension form.

Voltage-controlled voltammetry, i.e. with few ohmic drop, has allowed researchers to characterize voltage of each step at graphite electrolysis. Voltammetric oxidation of

HOPG near 2.0 V generated blisters which were seen by an optical microscope [16]. Voltammetry ranging from -2 to 3 V exfoliated graphite to produce functionalized graphenes used for primary battery electrodes [17]. Well-defined voltage control for reduction generated few-layer graphenes with the help of thermal expansion and ultrasonication [18]. Electrochemical intercalation of sodium dodecyl sulfate into graphite formed a stable colloidal graphene suspension of which properties were controlled by intercalation voltages [19]. HOPG electrochemically intercalated by mixtures of sulfuric and formic acids exfoliated to form CO blisters in which CO bubbles were trapped [20]. Although characteristic voltages have been addressed in these studies, a relationship between the formation of graphene oxide and the exfoliation has not been clarified yet from a viewpoint of electrode potential. A strategy of clarification is, first of all, to find how the oxidation of graphite alters the surface morphology at the intercalation.

We focus in this report on carrying out the strategy by voltammetric oxidation of the HOPG surface in basic solutions. The oxidized surface morphology, examined by means of STM, is expected to be related quantitatively with the oxidation charge. Questions are (i) whether graphite oxide is immobilized on the HOPG surface or not; (ii) what are geometry and uniformity of graphite oxide; (iii) how much is graphite oxide formed at a given potential; (iv) what are properties of graphite oxide such as conductivity and porosity. We aim at responding to these questions in this report.

Experimental

HOPG was purchased from Bruker Corp. Before each voltammetric run, the HOPG surface was exfoliated with adhesive tape. The capacitive current at a whole HOPG plate was much larger than that at a planar glassy carbon electrode with the same geometrical area. The extra-current is due to the large surface roughness at the edge of

the HOPG plate. In order to obtain a controlled area of an electrochemically active lamellar plane, a PTFE cylinder 6 mm in inner diameter was pressed on the exfoliated HOPG surface with the help of a gasket (o-ring). Voltammograms obtained in the cylindrical cell varied sometimes with the pressure between the cylinder and the HOPG. Another cell was an aqueous cylinder which was supported with surface tension between the aqueous solution and air. It was generated by expanding the aqueous solution sandwiched with the HOPG plate and a stainless steel plate, as illustrated in Fig. 1. The diameter of the cylinder was determined by a microscope.

Water used was distilled and then ion-exchanged. All the chemicals were of analytical grade. Ferrocenyl tetramethylammoniumhexafluorophosphate (FcTMA), was synthesized in house. FcTMA contained salt, mainly ammonium iodide, which was formed when iodide in ferrocenyl tetramethylammonium iodide was substituted for hexafluorophosphate. Accurate concentrations of FcTMA solutions were determined by voltammetric peak for the known value of the diffusion coefficient [21]. Water was deionized and distilled.

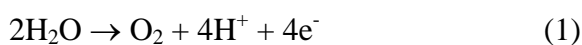
Cyclic voltammetry was carried out with a potentiostat, Compactstat (Ivium Tech., Netherlands). The reference electrode was Ag|AgCl in saturated KCl. The counter electrode was a platinum wire. Scanning tunneling microscope was NanoScope (MSE-FFAC001, Veeco).

3. Results and Discussion

3.1 Electrochemical oxidation of HOPG

The HOPG surface in cylindrical cell was oxidized in acidic and basic solutions by cyclic voltammetry with one cycle. The voltammograms in Fig. 2 show that the oxidation current rose up at 1.3 and 1.7 V, respectively in the NaOH and H₂SO₄

solutions. The iterative scan decreased slightly the anodic currents. The Tafel plot fell on a line for the current density over $5 \mu\text{A cm}^{-2}$. We designated the potential at the current density of $4 \mu\text{A cm}^{-2}$ in the Tafel plot as E_{TF} . Figure 3 shows dependence of E_{TF} on pH of the solution, where pH was varied by adding NaOH or H_2SO_4 to 0.1 M (= mol dm^{-3}) Na_2SO_4 solution. The increase in pH by 1 shifted E_{TF} by ca. 0.04 V, indicating that two electrons should be consumed for the oxidation of one hydrogen ion. The conventional oxidation of water, followed by



shows the 1:1 stoichiometry for H^+ (or OH^-) and e^- . This ratio fails to explain the present experimental dependence of E_{TF} on pH. More electrons should be generated than the oxidation of OH^- . A possible reaction generating more electrons is formation of carbocation [22-24] through



If it occurs in parallel with reaction (1), two electrons should generate in the consumption of one OH^- ion. The carbocation may soon react with dioxygen or water to yield an alcohol or an epoxy group. In order to support the participation of reaction (2), we made voltammetry at the platinum electrode under the same conditions as the voltammetry at the HOPG. The potential shift was 52 mV per pH at the Pt electrode, as shown in Fig. 3, i.e. corresponding to the one-electron oxidation. Therefore the two-electron reaction is specific to HOPG electrodes.

Values of the current density ranging from 20 to $250 \mu\text{A cm}^{-2}$ at a given potential varied with scan rates in the NaOH solution. They showed $v^{0.4}$ -dependence and $v^{0.1}$ -dependence at 1.2 V and potentials more than 1.3V, respectively. Since the order of v was less than, 0.5, the current should be controlled by some chemical and/or electrochemical kinetics rather than diffusion of OH^- . This supports the participation of

reaction (2), which belongs to a surface reaction.

The oxidized surface is predicted to be covered with graphite oxide, which is more hydrophilic than the HOPG surface. In order to verify the hydrophilicity, we measured contact angles of water drop on the HOPG surface which was oxidized in NaOH solution by one scan cyclic voltammetry at the scan rate, 10 mV s^{-1} , with several reverse potentials, E_r . The angle decreased at $E_r > 1.3 \text{ V}$, as shown in Fig. 4. This fact implies hydrophilic graphite oxide may be formed on the HOPG for $E_r > 1.3 \text{ V}$.

3.2 STM images of Oxidized Surface

Figure 5 shows STM photographs of the oxidized HOPG surfaces at three reverse potentials. The HOPG surface without the oxidation had no morphology within $0.5 \text{ }\mu\text{m}$ squares in magnification. Dots were found at potentials $E_r > 1.2 \text{ V}$. When the oxidation level was enhanced by an increase in E_r or a decrease in the scan rate, the number of dots were increased, keeping the size. The dots covered mostly the HOPG plane for $E_r > 1.5 \text{ V}$ (Fig. 5(C)). Therefore the anodic electrolysis generated the dots.

Figure 6 shows the magnified STM images of (A) the domain including the dots and (B) the flat domain in Fig. 5(A). The dots were an approximate circle ca. 15 nm in diameter, and were less than 20 nm . There were few overlaps of dots even at high density of the dots. The dots were formed heterogeneously, leaving behind the flat domain (Fig. 5(B)). The thickness of a dot was read by the STM current along a line traversing a dot. It was 0.5 nm in average and was less than 1 nm . Consequently, the dots are disk-shape with an aspect ratio less than 30:1. We call the dots nano-disks. The surface of the nano-disk was crumpled. It has been reported that the electrochemical oxidation of HOPG yielded shallow blisters on the surfaces [16,25]. The blisters are different from our nano-disks in that they take optical microscopic size and irregular size.

The STM current at a probe distinguishes obviously nano-disks from the flat HOPG plane. We took the ratio of the number of (x, y) digital points regarded as a nano-disk to all the sampled number. This ratio is equivalent to the ratio of the projected area of the nano-disks, S , to all the scanned area, $S_0 = (0.5 \mu\text{m})^2$. Figure 7 shows the variation of S/S_0 with the charge density of the oxidation, q . The area at a low oxidation level was proportional to q , whereas the ratio S/S_0 at a high level showed a constant, ca. 0.7. The proportionality indicates that nano-disks should disperse on the HOPG surface two-dimensionally without overlap. The two-dimensional dispersion is in accord with the uniformly flat disk form. The slope of the proportionality means the area generated by 1 C, or $2.2 \times 10^{-3} \text{ nm}^2$ per electron. This area is much smaller than the area of one carbon (0.026 nm^2) on a graphene sheet. The ratio, $0.026/0.0026 \approx 11$, indicates that a carbon atom relevant to formation of the nano-disks is oxidized by consumption of eleven electrons.

The constant value of S/S_0 (0.7) for $q > 50 \text{ C m}^{-2}$ in Fig. 7 shows that the nano-disks cannot cover the HOPG surface up by further oxidation. Since the nano-disks are not overlapped to get thicker by the further oxidation, the anodic charge more than $q > 50 \text{ C m}^{-2}$ may be consumed only by decomposition of water rather than by formation of the nano-disks. A reason for the limitation of $S/S_0 < 0.7$ is that no domain can be filled geometrically with random distribution of equi-sized disks without overlap.

3.3 Electrochemical properties

We characterize here electrochemical properties of the nano-disks by cyclic voltammetry and ac-impedance. Figure 8 shows voltammograms in 0.5 M KCl solution at the HOPG and the glassy carbon (GC) electrodes, and their oxidized electrodes at which the oxidation was made by cyclic voltammetry at $E_r = 1.5 \text{ V vs. Ag|AgCl}$ in 10

mM NaOH solution. The voltammetric currents in 0.5 M KCl solution are caused by the electric double layer capacitance because currents at $0.1 < E < 0.6$ V were proportional to the scan rates. The voltammograms at the oxidized HOPG (a2) was close to or less than that at the untreated HOPG (a1) for $E < 0.5$ V. Therefore the nano-disks do not increase the electroactive surface area although the surface gets geometrically rough. Possible reasons are electrical insulator of the nano-disks and/or no electric percolation of the nano-disks to the HOPG. In contrast, the oxidized GC electrode (b2) showed current density larger than the untreated GC (b1), as is well-known as the anodic activation of electrochemical pretreatments [26,27].

We examined electrochemical activity of the soluble redox species at the nano-disk coated electrode. The oxidized HOPG in 1 mM FcTMA + 0.5 M KCl aqueous solution showed the same voltammograms as those untreated HOPG, regardless of a degree of the anodic charge and scan rates for less than 0.1 V s^{-1} . FcTMA ought to react at the HOPG surface through nano-disks without any blocking. Therefore, the nano-disks are porous for transport of ions.

Electric double layer impedance of the oxidized HOPG was measured by the ac-impedance technique with 10 mV amplitude at the DC-potential (0.0 V) of the polarized potential domain in 0.5 M KCl solution. Figure 9 shows the Nyquist plots at the oxidized and untreated HOPG electrodes. The conventional model of the equivalent circuit for a double layer is a series combination of an ideal capacitance and a solution resistance. A Nyquist plot for this model shows theoretically a vertical line, whereas the experimental plots showed a line with the slope 11. When a capacitance, C , has frequency-dependence, the ac-current responding to ac-voltage, V , is formally expressed by [28,29]

$$I = \frac{d(CV)}{dt} = C \frac{dV}{dt} + V \frac{dC}{dt} = i\omega CV + V \frac{dC}{d\omega} \frac{d\omega}{dt} \quad (3)$$

where ω is the frequency of the ac-voltage. The term $(dC/d\omega)(d\omega/dt)$ in Eq. (3) is an in-phase component, or a conductance. Letting the inverse of the conductance, i.e. the resistance, be denoted as R_p , the equivalent circuit is a parallel combination of C and R_p . Then the impedance including the solution resistance, R_s , is represented by

$$Z_1 + iZ_2 = R_s + \frac{1}{1/R_p + i\omega C} \quad (4)$$

or

$$Z_1 - R_s = \frac{R_p}{1 + (\omega CR_p)^2}, \quad Z_2 = \frac{-\omega CR_p^2}{1 + (\omega CR_p)^2} \quad (5)$$

The experimental slope, 11, in Fig. 9 will be discussed later.

A quantitative relationship between double layer properties and a degree of the oxidation may be represented by the dependence of the capacitance on the area of projected nano-disks. By eliminating R_p from Eq. (4), the double layer capacitance can be represented by

$$C = \frac{-2Z_2}{\omega \{(Z_1 - R_s)^2 + Z_2^2\}} \quad (6)$$

The evaluated capacitance was proportional to $\ln(\omega)$ in the domain from 5 Hz to 50 kHz, as is consistent with at the platinum electrodes [28,29], and was empirically expressed as

$$C = k_1 - k_2 \ln \omega \quad (7)$$

for positive constants k_1 and k_2 . The frequency-dependence in C was rather small because of the logarithmic variation. Figure 10 shows variation of C at frequency 1 Hz with S/S_0 . The capacitance increased slightly with an increase in the oxidized area, indicating the enhancement of the conducting area with an increase in the oxidation degree. It approached a constant value for $S/S_0 > 0.35$, and did not vary any more. Consequently, the nano-disks themselves do not participate in electrical conduction, but

may generate simply surface roughness of the HOPG substrate. The invariance of C is consistent with the electric insulator of the nano-disks in Fig. 8. This behavior is in contrast with the oxidized GC electrodes [26,27].

Taking the ratio of the two equations in Eq. (5) yields

$$-Z_2/(Z_1 - R_s) = \omega R_p C \quad (8)$$

By inserting Eq. (8) into the definition $1/R_p = (dC/d\omega)(d\omega/dt)$ in Eq. (3) and using the relation $\omega t = 2\pi$ (e.g. $e^{i\omega t} = 1$), we have $R_p = 2\pi/k_2\omega$. Therefore, Eq. (8) is almost constant for frequency variations. This interpretation agrees with a given slope of the line in Fig. 9. Values of the slopes did not vary not only with frequency but also S/S_0 . Therefore the formation of the nano-disks has no effect on the quality of the double layer.

It is interesting to deduce a possibility of generating uniform sized nano-disks without overlap. Since the basal plane of HOPG is stabilized by graphene-like crystal structure, formation of carbocations needs high activation energy or overpotential. Once carbocation is generated at any point on the surface overcoming the overpotential, it deforms the surrounding crystal structure to decrease the activation energy. Therefore carbocations are formed closely each other. They react with oxygen to yield clusters of graphite oxides. Since the density per area of the cluster is lower than that of graphite, the cluster cannot bound with crystal structure. Then it protrudes from the crystal surface to form disks, associated with wrinkles. Since it is an electrical insulator, it has no effect on further oxidation.

4. Conclusion

The defects of the HOPG crystal structure by the oxidation are different from the intercalated graphene in that

(a) the top layer of the oxidized HOPG is hydrophilic, indicating the absence of

hydrophobic graphene layer (in Fig. 4);

(b) the extra-oxidation charge does not enhance the amount of the defects (in Fig. 7);

(c) nano-disks are dispersed heterogeneously on the planar HOPG;

(d) the electric conduction specific to graphene layers is lost on the nano-disks (in Fig. 8),

(e) the nano-disks are so porous for ions that the electrode reaction is not blocked; and

(f) the double layer capacitance is almost independent of the oxidation level.

These deviations from the conventional image, however, do not always controvert the intercalation if

(g) the applied potentials and/or the current density are insufficient to cause the intercalation, and if

(h) the anodic intercalation may occur less frequently than the cathodic one.

Our answer to the questions in Introduction is

(i') generated graphite oxide is immobilized on the HOPG surface;

(ii') it takes disk-shape 15 nm in diameter with 30:1 aspect ratio;

(iii') the generated amount is restricted up to the surface coverage

(iv') graphite oxide is electric insulated and porous for ions and solvent, and consequently it has no effect of reactions of foreign redox species, or few effect on double layer capacitance.

Acknowledgements

This work was financially supported by Grants-in-Aid for Scientific Research (Grant 22550072) from the Ministry of Education in Japan.

References

[1] L. Staudenmaier, Ber. Dtsch. Chem. Ges. 31 (1898) 1481.

-
- [2] H.C. Schniepp, J.L. Li, M.J. McAllister, H. Sai, M. Herrera-Alonso, D.H. Adamson, R.K. Prud'homme, R. Car, D.A. Saville, I.A. Aksay, J. Phys. Chem. B 110 (2006) 8535–8539.
- [3] S. Pan, I.A. Aksay, ACS Nano 5 (2011) 4073–4083.
- [4] S. Stankovich, D.A. Dikin, G.H. Dommett, K.M. Kohlhaas, E.J. Zimney, E.A. Stach, R.D. Piner, S.T. Nguyen, R.S. Ruoff, Nature 442 (2006) 282–286.
- [5] V.V. Singh, D. Joung, L. Zhai, S. Das, S.I. Khondaker, S. Seal, Prog. Mater. Sci. 56 (2011) 1178–1271.
- [6] D.R. Dreyer, S. Park, C.W. Bielawski, R.S. Ruoff, Chem. Soc. Rev. 39 (2010) 228–240.
- [7] W.S. Hummers, R.E. Offeman, J. Am. Chem. Soc. 80 (1958) 1339.
- [8] C.T.J. Low, F.C. Walsh, M.H. Chakrabarti, M.A. Hashim, M.A. Hussain, Carbon 54 (2013) 1–21.
- [9] A. Jnioui, A. Metrot, A. Storck, Electrochim. Acta, 27 (1982) 1247–1252.
- [10] Y. Takada, R. Fujii, Tanso, 122 (1985) 110–113.
- [11] H. Takenaka, M. Kawaguchi, M. Lerner, N. Bartlett, J. Chem. Soc. Chem. Commun. (1987) 1431–1432.
- [12] M. Inagaki, N. Iwashita, Z.D. Wang, Y. Maeda, Synth. Met. 26 (1988) 41–47.
- [13] M. Noel, R. Santhanam, M.F. Flora, J. Appl. Electrochem. 24 (1994) 455–459.
- [14] M. Toyoda, A. Shimizu, H. Iwata, M. Inagaki, Carbon, 39 (2001) 1697–1707.
- [15] Y. Soneda, M. Toyoda, Y. Tani, J. Yamashita, M. Kodama, H. Hatori, M. Inagaki, J. Phys. Chem. Solid, 65 (2004) 219–222.
- [16] K.W. Hathcock, J.C. Brumfield, C.A. Goss, E.A. Irene, R.W. Murray, Anal. Chem. 67 (1995) 2201–2206.
- [17] D. Wei, L. Grande, V. Chundi, R. White, C. Bower, P. Andrewa, Chem. Commun. 48 (2012) 1239–41.
- [18] G.M. Morales, P. Schifani, G. Ellis, C. Ballesteros, G. Martinez, C. Barbero, H.J. Salavagione, Carbon, 49 (2011) 2809–16.

-
- [19] M.Alanyalioglu, J.J. Segura, J. Oro-Sole, N.Casan-Pastor, Carbon, 50 (2012) 142-152.
- [20] E. Bourelle, B. Claude-Montigny, A. Metrot, Mol. Cryst. Liq. Cryst. 310 (1998) 321-326.
- [21] H. Zhang, K. Aoki, J. Chen, T. Nishiumi, H. Toda, E. Torita, Electroanalysis, 23 (2011) 947-952.
- [22] M. Galicia, F.J. González, J. Electrochem. Soc. 149 (2002) D46-D50.
- [23] C.P. Andrieux, F. Gonzalez, J.-M.Saveant, J. Electroanal. Chem. 498 (2001) 171–180.
- [24] L.S.H.-Munoz, R.J.F.-Soriano, C.V.-Lopez, E. Klimova, L.A.O.-Frade, P.D. Astudillo, F.J. Gonzalez, J. Electroanal. Chem. 650 (2010) 62–67.
- [25] C.A. Goss, J.C.Brumfield, E.A. Irene, R.W. Murray, Anal. Chem. 65 (1993) 1378-1389.
- [26] R.L.McCreery, In Electroanalytical Chemistry; A.J. Bard, Ed.; Dekker, New York, 1991; Vol. 17.
- [27] R.L. McCreery, Chem. Rev. 108 (2008) 2646–2687.
- [28] K. Aoki, Y. Hou, J. Chen, T. Nishiumi, J. Electroanal. Chem. 689 (2013) 124-129.
- [29] Y. Hou, K.J. Aoki, J. Chen, T. Nishiumi, Univ. J. Chem. 1 (2013) 162-169.

Figure Captions

Figure 1. Illustration of the cell of the aqueous cylinder pulled with both the HOPG plate and the stainless steel plate.

Figure 2. Cyclic voltammograms in (a) 10 mM NaOH + 100 mM Na₂SO₄ solution and (b) 1 M H₂SO₄ solution at the HOPG electrode for the scan rate, 10 mV s⁻¹.

Figure 3. Variations of E_r with pH obtained at the (circles) HOPG and the (triangles) platinum electrode in various pH solutions at $\nu = 10 \text{ mV s}^{-1}$, where E_{TF} is satisfied with the Tafel equation, $E = E_{TF} + a \log(I/\mu\text{A})$.

Figure 4. Variation of contact angles of water drop on the HOPG surface with E_r in 10 mM NaOH solution.

Figure 5. STM photographs in $(500 \text{ nm})^2$ of the HOPG surface oxidized in the NaOH solution by cyclic voltammetry with $E_r =$ (A) 1.20, (B) 1.25 and 1.30 V vs. Ag|AgCl for $\nu = 10 \text{ mV s}^{-1}$.

Figure 6. STM images of the HOPG surface oxidized at 1.2 V, which include (A) some nano-disks at a magnification of $(100 \text{ nm})^2$ and (B) the flat domain of Fig. 5(A) at a magnification of $(10 \text{ nm})^2$.

Figure 7. Dependence of the normalized area of nano-disks on the anodic charge density.

Figure 8. Cyclic voltammograms at $\nu = 10 \text{ mV s}^{-1}$ in 0.5 M KCl solution at (a1) the HOPG, (a2) the HOPG oxidized at $E_r = 1.5 \text{ V}$ in 10 mM NaOH + 100 mM Na₂SO₄ solution, (b1) the GC, and (b2) the GC oxidized at $E_r = 1.5 \text{ V}$ in the above solution,

Figure 9. Nyquist plots in 0.5 M KCl solution at (circles) the bare HOPG and (triangles) the HOPG oxidized at $E_r = 1.5 \text{ V}$.

Figure 10. Variation of the capacitance at 1 Hz with the normalized area of the nano-disks.

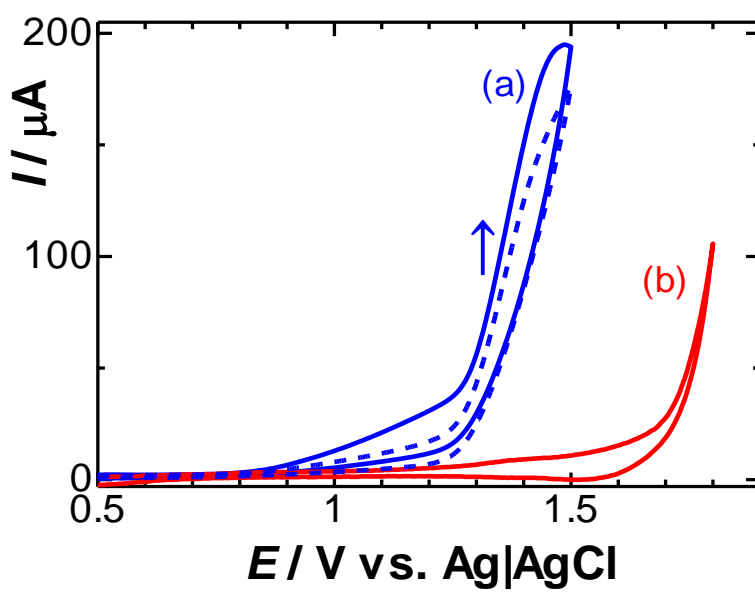
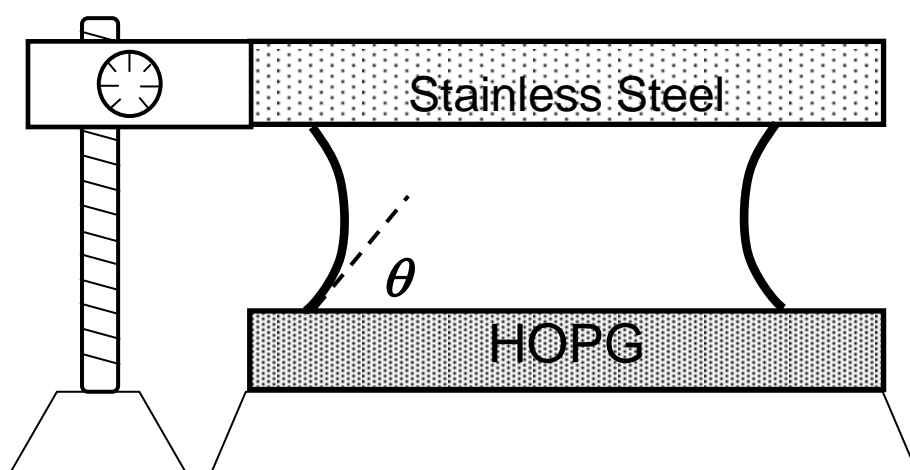


Fig. 2

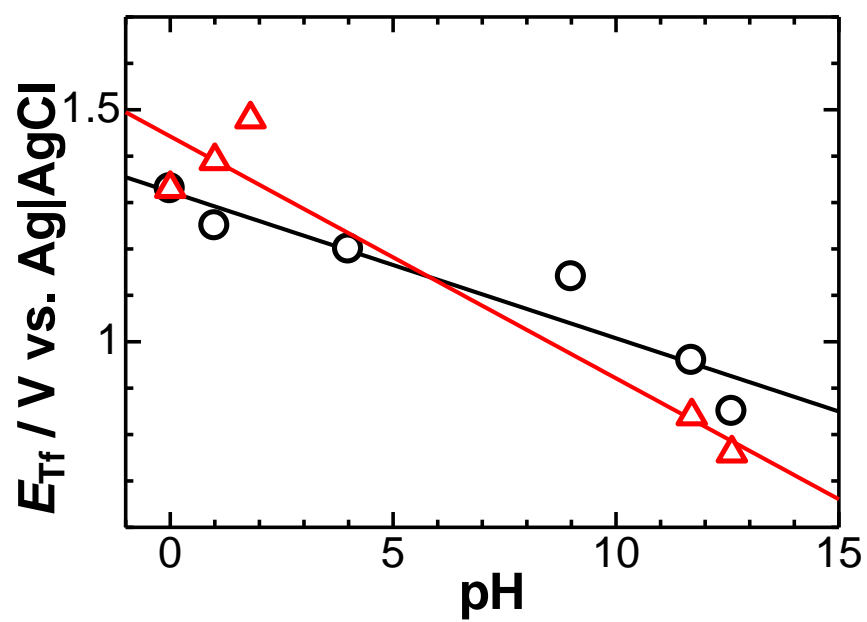


Fig. 3

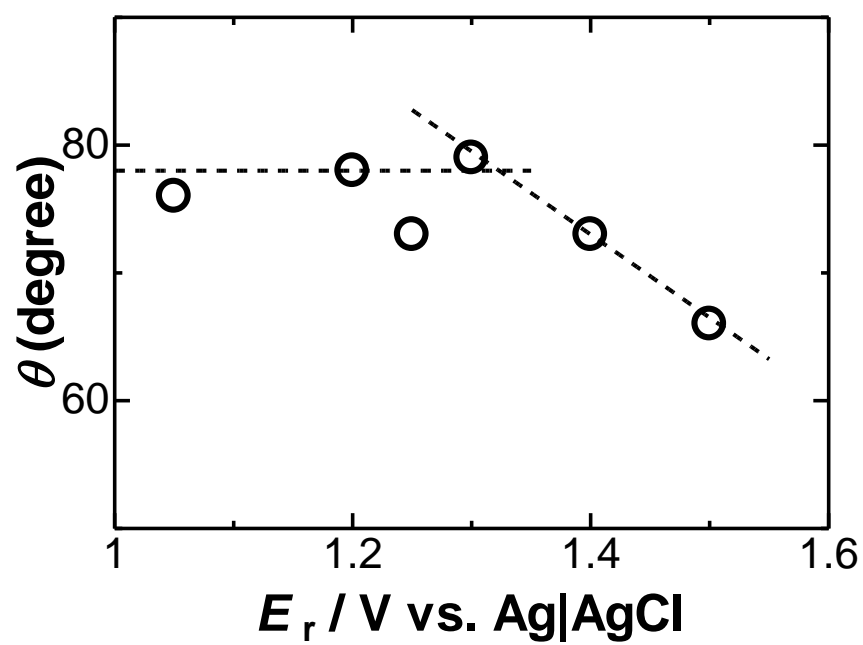


Fig. 4

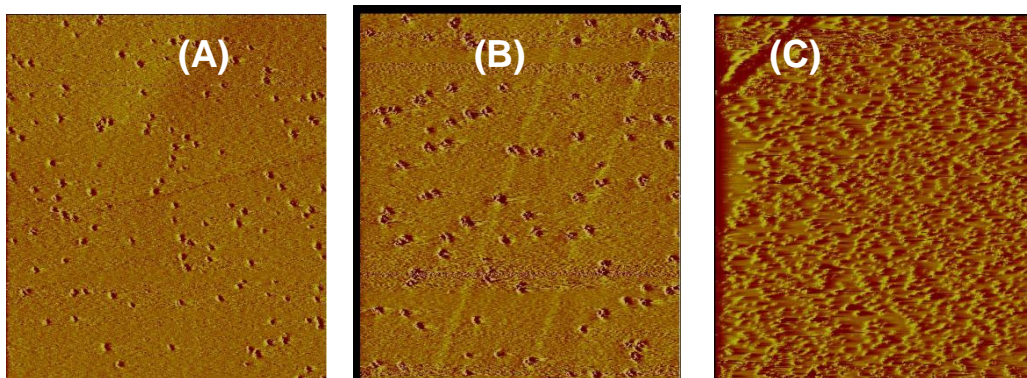


Fig. 5

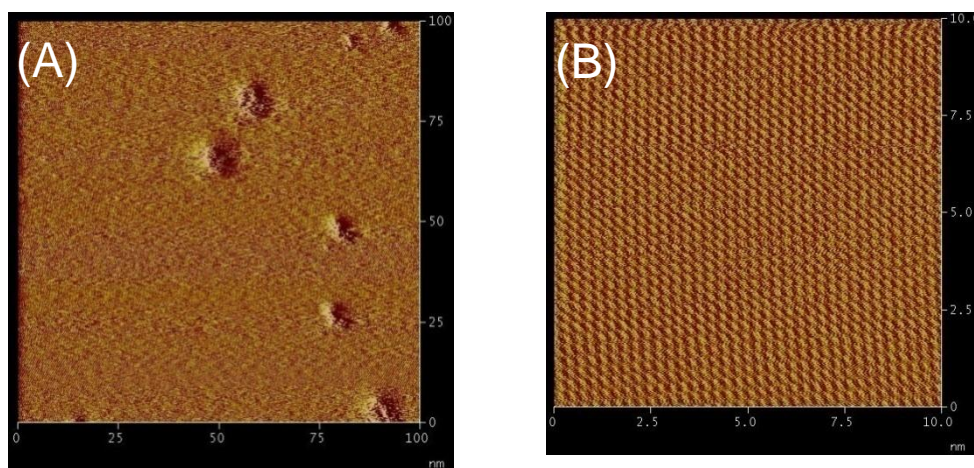


Fig. 6

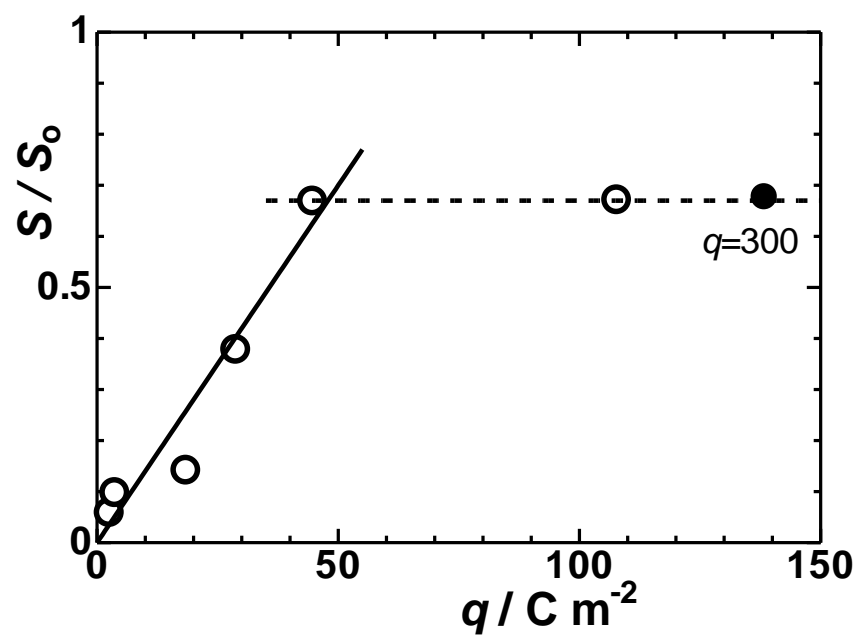


Fig. 7

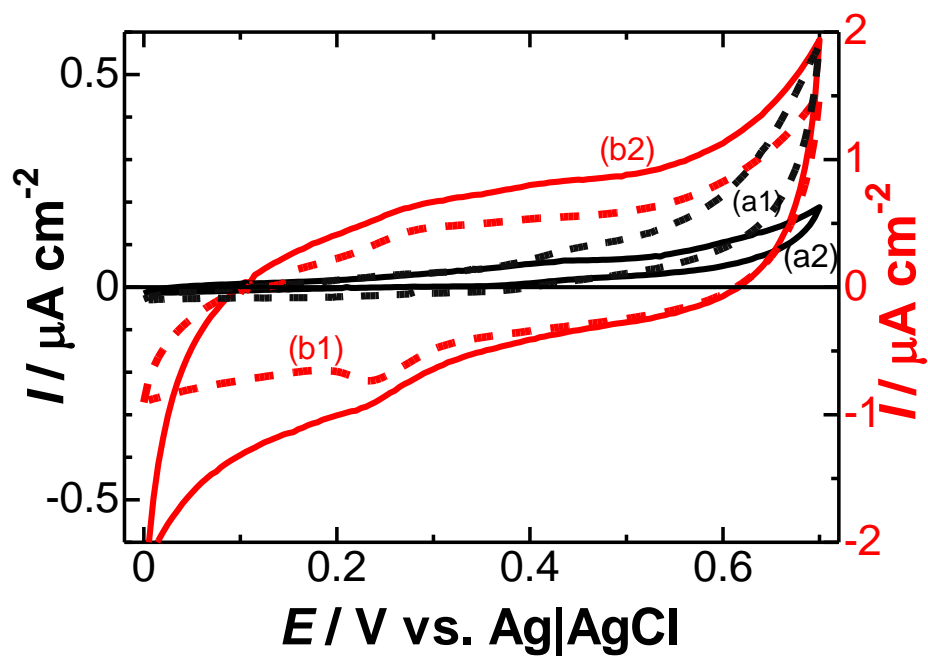


Fig. 8

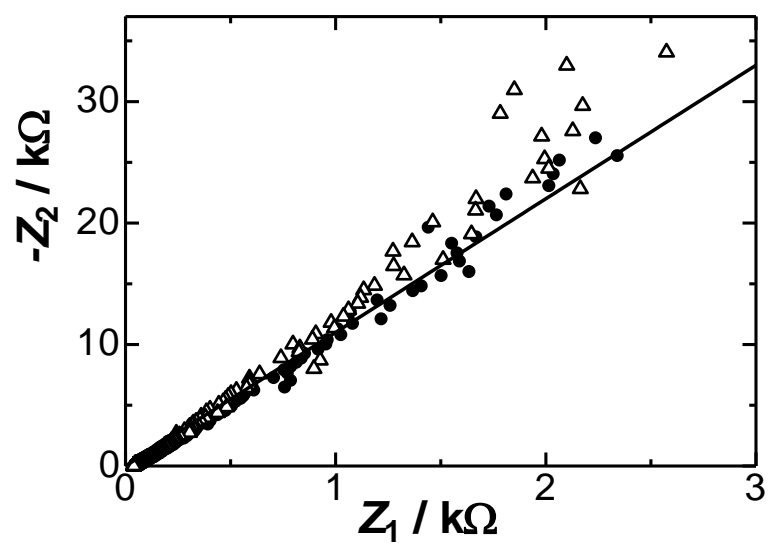


Fig. 9

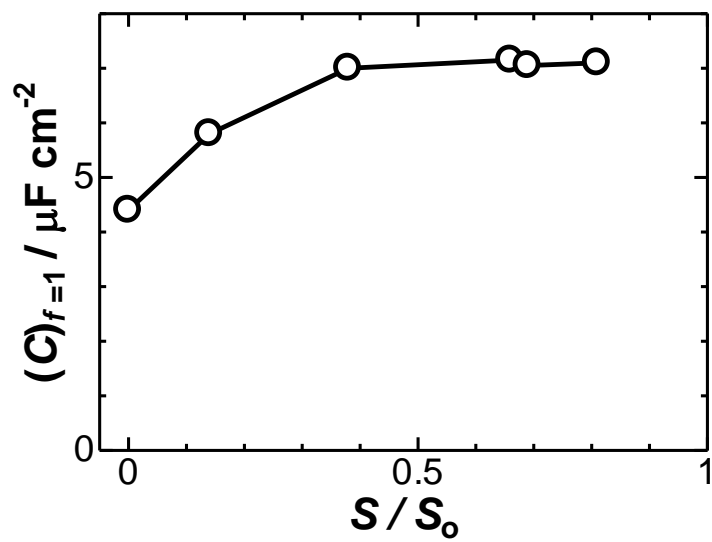


Fig. 10

Nano-disks of graphene oxide is formed on the HOPG surface by electrooxidation. They are 15 nm in diameter, an electrical insulator, and surface-bound material. They are different from the conventional view of the intercalation.